

Scattering of low- to intermediate-energy positrons from molecular hydrogen

David D. Reid, William B. Klann

*Department of Physics and Astronomy,
Eastern Michigan University, Ypsilanti, MI 48197*

J. M. Wadehra

*Department of Physics and Astronomy,
Wayne State University, Detroit, MI 48202*

(Date textdate; Received textdate; Revised textdate; Accepted textdate; Published textdate)

Abstract

Using a complex model potential, we have calculated the total, integrated elastic, momentum transfer, absorption, and differential cross sections for positrons scattered from molecular hydrogen. The widely available software package GAUSSIAN is used to generate the radial electronic charge density of molecule which is used to produce the interaction potentials. The quasifree absorption potential, previously developed and used for positron-atom scattering, is extended to positron scattering from molecular targets. It is shown that this model potential approach produces accurate results even into the low-energy regime.

I. INTRODUCTION

The scattering of positrons from atomic and molecular targets continues to be an area of active investigation in both experimental and theoretical collision studies. As the ability to produce controlled positron beams continues to be refined, and such beams become available in more laboratories, a larger variety of positron-gas systems are being studied experimentally with improving results. The state of theoretical calculations in this area can be divided into four impact-energy (E) regimes. These are very low energy ($E \lesssim 0.1$ eV), low energy ($0.1 \text{ eV} < E < E_{Ps}$) where E_{Ps} is the threshold for positronium formation, intermediate energy ($E_{Ps} < E < 1000$ eV), and high energy ($E > 1000$ eV) regimes. Low and very low energy calculations are typically performed at the *ab initio* level rather than with model potentials partly because in this energy regime one does not have to take into account several inelastic channels which are complicated to handle exactly [1]. Furthermore, calculations using model potentials have performed only moderately well or even poorly at lower energies because the projectile spends more time near the target causing the results to be more sensitive to the details of the interaction. However, the reverse is true at intermediate energies. Because of the predominance of many inelastic processes, particularly positronium formation, electronic excitation, and ionization, calculations at the *ab initio* level become extremely difficult. Also, in this energy regime, high-energy approximations, such as Born-Bethe theory, cannot yet be trusted.

We will show in this paper that use of complex model potentials can produce accurate intermediate-energy results even for positron-molecule scattering, as they have for the scattering of both electrons and positrons in atomic gases [2]. However, despite the success of this approach for atomic targets at intermediate energies, use of model potentials runs into difficulties that limited their applicability to molecular targets. First, the generation of molecular charge densities is substantially more difficult than the generation of atomic charge densities; therefore, many of the previous calculations for molecules employed the independent-atom model [3, 4] in which the scattering process from a molecule is treated by combining the scattering processes from the individual atoms that make up the molecule. This approach necessarily breaks down at lower energies, depending on the geometry of the molecule, because when the de Broglie wavelength of the incident positrons is on the order of the size of the bond lengths between the atoms in the molecule they cannot possibly “see”

the molecule as a set of individual atoms. Furthermore, model potentials that assume that the electrons of the target atom can be treated as a free electron gas are not accurate for atomic hydrogen containing only one electron. Therefore, in this case, the independent atom approximation for molecules containing the hydrogen atom is not expected to be very good. Second, no good model absorption potential specifically designed for positron scattering has existed until only recently [5]. Having no viable option, previous positron-molecule collision calculations were carried out either using model absorption potentials that were designed for electron scattering, or modifying those electron absorption potentials in purely empirical ways [6].

Because of the issues just described, and despite the fact that electron scattering from molecular hydrogen is a well-studied problem, to the best of our knowledge, there are only two published calculations of total cross sections for positron scattering from H_2 at intermediate impact energies [4, 6]. In this paper, we study positron- H_2 scattering in a way that addresses both of the difficulties discussed in the previous paragraph. First, as will be discussed in more detail below, the present calculations use *molecular* charge densities to calculate the model potentials. By doing so, we bypass all of the issues concerning use of the independent-atom model. As a result, not only are we able to obtain good cross section results for scattering from H_2 at intermediate impact energies, but, surprisingly, our results are also quite good well into the low-energy regime. Second, we demonstrate the successful extension of the quasifree model absorption potential developed for positron-atom scattering to the scattering of positrons from molecular targets. Using a more appropriate positron absorption potential gives better overall results with much less need for empiricism.

This paper is organized into four parts. Following the present introductory remarks, we explain in section II the theoretical framework for our calculations. First, in subsection II.A, we describe the interaction potentials used and discuss the relevant issues concerning the extension of the quasifree model to molecular targets. Subsection II.B is devoted to a discussion of how we generated the molecular charge densities (and static potential) of the target using the commercially available software GAUSSIAN [7]. The details of how these calculations were performed are then given in subsection II.C. In section III, we present our results for total, integrated elastic, momentum transfer, absorption, and differential cross sections from low to intermediate impact energies. Finally, we make some concluding remarks in section IV. Unless otherwise specified, we use atomic units ($\hbar = e = m_e = 1$)

throughout this paper.

II. THEORY

A. Interaction Potentials

In the present calculations we model the positron-target system by a complex interaction potential, $V(r)$, that consists of three parts. These parts are the static potential $V_{st}(r)$, the polarization potential $V_{pol}(r)$, and the absorption potential $V_{abs}(r)$, such that

$$V(r) = V_{st}(r) + V_{pol}(r) + iV_{abs}(r). \quad (1)$$

Each interaction potential is determined by the radially averaged electron charge density of the target molecule, $\rho(r)$, which is obtained using the method discussed in subsection II.B below. The static potential is given by

$$V_{st}(r) = \left\langle \frac{Z}{|\mathbf{r} - \mathbf{b}|} \right\rangle - 4\pi \int_0^\infty \frac{\rho(r')}{r_>} r'^2 dr', \quad (2)$$

where Z is the number of protons of the target ($Z = 2$ in the present case), \mathbf{b} is a vector that points from the center of the molecule to a nucleus, and $r_>$ is the larger of r and r' .

Following De Fazio *et al* [8], the polarization interaction is given, in terms of the electron density, as

$$V_{pol}(r) = -D_4(r) \frac{\alpha_d}{2r^4} - D_6(r) \frac{\alpha_q}{2r^6} - D_8(r) \frac{\alpha_o}{2r^8} \quad (3)$$

where α_d , α_q , and α_o are the dipole, quadrupole, and octopole polarizabilities of the target molecule, respectively. In Table I, the values of the polarizabilities and their sources, as well as other parameters used in these calculations are provided. In Eq. (3) the functions $D_{2\ell+2}(r)$ are damping functions whose purpose is to guarantee that $V_{pol} \rightarrow 0$ as $r \rightarrow 0$; these functions are given by

$$D_{2\ell+2}(r) = \frac{\int_0^r \rho(r') r'^{2\ell+2} dr'}{\int_0^\infty \rho(r') r'^{2\ell+2} dr'}. \quad (4)$$

The absorption potential used in this work is an extension of the quasi-free model for positron-atom scattering that was given in our previous work [5]. The form of this interaction potential is

$$V_{abs} = -\frac{1}{2}\rho\bar{\sigma}_b v, \quad (5)$$

where v is the local speed of the incident positron and $\bar{\sigma}_b$ is the average cross section for binary collisions between the positron and the electrons of the target molecule. One of the important aspects of the present study is to formulate an extension of this model interaction potential to the case of molecular targets. Besides the electron density, the only other target-dependent quantity used in the absorption potential is the energy gap Δ . Within the quasifree binary collision model, Δ plays a dual role as both (a) the energy gap between the initial state and the final energy state of the originally bound electron, and (b) the lowest energy threshold for inelastic processes. For *electron*-atom scattering, these two roles are consistent with each other if Δ is set equal to the excitation threshold (E_{exc}) of the target atom. However, for *positron*-atom scattering the formation of positronium introduces another inelastic threshold which can be lower than the threshold for excitation. As an example, for positron scattering from alkali-metal atoms the threshold for positronium formation (E_{Ps}) is zero [13]. In the quasifree model the absorption cross section diverges as $\Delta \rightarrow 0$. Thus, for many positron-atom systems one has to find a reasonable choice for Δ that will be sufficiently close to the true inelastic threshold so as to minimize the absence of low-energy absorption in the calculations, but not so small that cross sections begin to diverge. Our previous investigations of positron-atom scattering [5, 13] have suggested that the appropriate choice for Δ is to set it equal to the lowest *nonzero* inelastic threshold.

In the case of positron scattering from molecular targets the inelastic threshold is effectively always open because of rovibrational excitation thresholds of the target molecules. Besides the rovibrational modes, the possibility of the dissociation of the molecule adds an additional inelastic process with threshold E_{diss} . In the derivation of the quasifree model, the only inelastic processes that are considered are those that can result from a binary collision between the incident positron and a target electron, namely, electronic excitation and ionization by positron impact, and positronium formation. Obviously, rovibrational excitation and dissociative processes are not part of the binary collision. This would most directly suggest that the energy gap be set equal to E_{Ps} . However, the above considerations must be balanced against the other role of Δ as the threshold at which *any* inelastic scattering occurs. Therefore, in the present study we have taken Δ to equal the average of E_{Ps} and

the threshold of disscociation,

$$\Delta = \frac{1}{2}(E_{Ps} + E_{diss}) . \quad (6)$$

For positron scattering the binary collision cross section $\bar{\sigma}_b$ of Eq.(5) is given by [5, 13],

$$\bar{\sigma}_b = \frac{\pi}{(\varepsilon E_F)^2} \begin{cases} f(0) & \varepsilon^2 - \delta \leq 0 \\ f(\sqrt{\varepsilon^2 - \delta}) & 0 < \varepsilon^2 - \delta \leq 1 , \\ f(1) & 1 < \varepsilon^2 - \delta \end{cases} \quad (7)$$

where

$$f(x) = \frac{2}{\delta}x^3 + 6x + 3\varepsilon \ln\left(\frac{\varepsilon - x}{\varepsilon + x}\right) \quad (8)$$

and

$$\delta = \frac{\Delta}{E_F}, \quad \varepsilon = \sqrt{\frac{E}{E_F}}. \quad (9)$$

The quantities $E_F = \hbar^2 k_F^2 / 2m$ and $k_F = (3\pi^2 \rho)^{1/3}$ are the Fermi energy and the Fermi wavenumber (or momentum) corresponding to the target radial electron density ρ .

B. The Electronic Charge Density

In the present calculations, the electronic charge density in the hydrogen molecule is calculated with GAUSSIAN [7] using the full configuration interaction method with both single and double substitutions [14]. This code is now fast and readily available. Using the `cube=density` command in GAUSSIAN, we first generated the electronic charge density $\rho(\mathbf{r})$ on a sufficiently large three-dimensional cubic grid to cover the needed range of the calculation with a step size of 0.04 a_0 in each direction. By interpolation [15], we then obtained values of $\rho(\mathbf{r})$ over the surface of a sphere of radius r centered upon the geometric center of the molecule; Fig. 1 illustrates this procedure. For visual clarity, Fig. 1 only shows points on a plane; in fact, the symmetry of H_2 only requires generation of $\rho(\mathbf{r})$ over one quadrant of such a plane. The value of the radial charge density at r is then calculated by numerical integration

$$\rho(r) = \frac{1}{4\pi} \int_0^{2\pi} \int_0^\pi \rho(\mathbf{r}) \sin \theta \, d\phi d\theta. \quad (10)$$

In this manner, values of $\rho(r)$ are calculated for every value of r needed in the integration of the radial Schrödinger equation to be discussed in the next subsection.

C. Calculations

For the spherically symmetric potential of Eq. (1) the scattering process is symmetric about the direction of the incident positron. The solution $u_\ell(r)$, therefore, is generated by the radial Schrödinger equation (in atomic units)

$$\left[\frac{d^2}{dr^2} - \frac{\ell(\ell+1)}{r^2} + 2[E - V(r)] \right] u_\ell(r) = 0 \quad (11)$$

where $E = \hbar^2 k^2 / 2m$ is the impact energy of the collision and ℓ is the angular momentum quantum number which also represents the order of the partial wave [16].

Equation (11) is integrated out to a distance of 10 bohr radii from the center of the molecule via the Numerov technique [17]. The first 51 ($\ell_{\max} = 50$) phase shifts are calculated exactly by comparing u_ℓ , the radial wave function of the target plus positron system, at two adjacent points r and $r_+ = r + h$:

$$\tan(\delta_\ell) = \frac{r_+ u_\ell(r) j_\ell(kr_+) - r u_\ell(r_+) j_\ell(kr)}{r u_\ell(r_+) n_\ell(kr) - r_+ u_\ell(r) n_\ell(kr_+)}, \quad (12)$$

where h is the step size ($h = 0.00075 a_0$) of the calculation, and j_ℓ and n_ℓ are the spherical Bessel and Neumann functions evaluated using the algorithm of Gillman and Fiebig [18].

The scattering amplitude is obtained from the phase shifts by

$$f(\theta) = \frac{1}{2ik} \sum_{\ell=0}^{\ell_{\max}} (2\ell+1) (\exp(2i\delta_\ell) - 1) P_\ell(\cos\theta) + f_4(\theta) + f_6(\theta) + f_8(\theta). \quad (13)$$

The functions f_4 , f_6 , and f_8 are the higher- ℓ contributions from the Born phase shifts for the dipole ($\sim 1/r^4$), quadrupole ($\sim 1/r^6$), and octopole ($\sim 1/r^8$) parts of the asymptotic polarization potential, respectively. The closed form expressions for these functions are [19]

$$f_4(\theta) = -\pi k \alpha_d \left(\frac{\sin(\theta/2)}{2} + \sum_{\ell=0}^{\ell_{\max}} \frac{P_\ell(\cos\theta)}{(2\ell+3)(2\ell-1)} \right), \quad (14)$$

$$f_6(\theta) = -3\pi k^3 \alpha_q \left(-\frac{\sin^3(\theta/2)}{18} + \sum_{\ell=0}^{\ell_{\max}} \frac{P_\ell(\cos\theta)}{(2\ell+5)(2\ell+3)(2\ell-1)(2\ell-3)} \right), \quad (15)$$

and

$$f_8(\theta) = -10\pi k^5 \alpha_o \left(\frac{\sin^5(\theta/2)}{450} + \sum_{\ell=0}^{\ell_{\max}} \frac{P_\ell(\cos\theta)}{(2\ell+7)(2\ell+5)(2\ell+3)(2\ell-1)(2\ell-3)(2\ell-5)} \right). \quad (16)$$

Once the scattering amplitude is known, the various cross sections can be determined. The total cross sections which include both elastic and inelastic scattering, are obtained from the forward scattering amplitude by

$$\sigma_{tot} = \frac{4\pi}{k} \text{Im} [f(0)] . \quad (17)$$

The cross sections for elastic scattering are found by integrating the scattering amplitude

$$\sigma_{elas} = 2\pi \int_0^\pi |f(\theta)|^2 \sin \theta d\theta . \quad (18)$$

The absorption cross sections (the cross section for inelastic scattering) are determined by the difference

$$\sigma_{abs} = \sigma_{tot} - \sigma_{elas} . \quad (19)$$

The differential cross sections for the angular distribution of the scattered wave are given by

$$\frac{d\sigma}{d\Omega} = |f(\theta)|^2 . \quad (20)$$

Finally, the momentum transfer cross sections are found using

$$\sigma_{mom} = 2\pi \int_0^\pi (1 - \cos \theta) |f(\theta)|^2 \sin \theta d\theta . \quad (21)$$

III. RESULTS

Figure 2 shows the present results of the total cross sections for the scattering of positrons by H₂ compared with several experimental measurements. To the best of our knowledge, no other theoretical calculations of total cross sections have been able to predict the structure in this curve over as large a range of positron energies as in the present calculations. These structures extending across the low- to intermediate-energy ranges are accurately reproduced. The present results correctly predict the local minimum in the low-energy regime near 4 eV and the local maximum in the intermediate-energy regime near 25 eV. In the range of around 9 eV to 11 eV the present results stray outside of the error bars, overestimating the experimental values. However, in this connection, it should be noted that cross section measurements are expected to be underestimated due to the inability to discriminate projectiles elastically scattered through small angles [20]. To get the best indication of the quality of the present calculations, the error bars shown in Fig. 2 are the "maximum errors"

as reported in Refs. [20, 21] and not just the statistical uncertainties. Error bars for the other experimental data are not shown as the errors reported were not of comparable detail.

In Fig. 3, we show our absorption cross section results compared to estimates based on various measurements. The experimental points are a combination of different experiments for measurements made at common, or nearly common, impact energies. The present results show good agreement with the experimental cross sections in the region of overlap. The fact that our results overestimate the experimental points at every energy is to be expected because the ionization cross sections are only for first ionizations, the excitation cross sections only account for excitations to the $B^1\Sigma$ state, and there is no experimental data added for other processes (although they are expected to be small at these energies). As one would expect, the absorption cross sections are quite sensitive to the absorption potential; the fact that we have such good results for this partial cross section, confirms the applicability of the quasifree model for molecular targets.

Our demonstration, in Figs. 1 and 2, that the present total and absorption cross sections are good also confirms the quality of our integrated elastic cross sections at intermediate energies. In Table II, we provide the values of our differential, integrated elastic, and momentum transfer cross sections at intermediate impact energies. As mentioned in sec. I, we can also claim that the present model potential results are reliable well into the low-energy regime. This is confirmed partly by the quality of the low-energy total cross sections in Fig. 2. However, a much more stringent test is made by differential cross sections. To date, there are no measurements of differential cross sections for positron scattering from H_2 . Thus, in Fig. 4, we compare our present low-energy differential cross sections against the *ab initio* calculations of Lino *et al* using the Schwinger multichannel method [1]. Despite the fact that, at small scattering angles, our calculations show a slight dip, the present results show excellent agreement with their calculations at every energy for which a comparison has been made.

IV. CONCLUSIONS

In the present calculations, we have presented calculations of scattering cross sections for positrons scattered from H_2 . Using a single model potential approach, we have presented accurate total cross sections through both the low- and intermediate-energy regimes correctly

matching the detailed structure in this curve. To the best of our knowledge, this is the first theoretical calculation to achieve this feat. We have also demonstrated that, with a very minor modification, the positron quasifree absorption potential can perform equally well, or better, for scattering in molecular gases as it has in atomic gases. Furthermore, we have introduced a simple scheme for obtaining accurate molecular charged densities using GAUSSIAN that can be applied to almost any molecule bypassing the need for the independent atom model.

Acknowledgments

We wish to thank H. B. Schlegel and M. C. Milletti for recommending the use of GAUSSIAN for calculating molecular charge densities. We also acknowledge G. Maroulis and D. M. Bishop for advise concerning the polarizabilities of H_2 . The assistance of C. M. Surko and J. P. Marler with their values of the excitation cross sections is greatly appreciated. Completion of this research was made possible by a Spring-Summer research award from Eastern Michigan University.

- [1] J. L. S. Lino, J. S. E. Germano, E. P. da Silva, and M. A. P. Lima, *Phys. Rev. A* **58**, 3502 (1998).
- [2] D. D. Reid and J. M. Wadehra, *Phys. Rev. A* **50**, 4859 (1994).
- [3] D. D. Reid and J. M. Wadehra, *Chem. Phys. Lett.* **311**, 385 (1999).
- [4] R. Raizada and K. L. Baluja, *Phys. Rev. A* **55**, 1533 (1997).
- [5] D. D. Reid and J. M. Wadehra, *J. Phys. B* **29**, L127 (1996); *B* **30**, 2318 (1997).
- [6] K. L. Baluja and A. Jain, *Phys. Rev. A* **45**, 7838 (1992).
- [7] Gaussian 98 (Revision A.11), M. J. Frisch, G. W. Trucks, H. B. Schlegel, G. E. Scuseria, M. A. Robb, J. R. Cheeseman, V. G. Zakrzewski, J. A. Montgomery, R. E. Stratmann, J. C. Burant, S. Dapprich, J. M. Millam, A. D. Daniels, K. N. Kudin, M. C. Strain, O. Farkas, J. Tomasi, V. Barone, M. Cossi, R. Cammi, B. Mennucci, C. Pomelli, C. Adamo, S. Clifford, J. Ochterski, G. A. Petersson, P. Y. Ayala, Q. Cui, K. Morokuma, D. K. Malick, A. D. Rabuck, K. Raghavachari, J. B. Foresman, J. Cioslowski, J. V. Ortiz, B. B. Stefanov, G. Liu, A. Liashenko, P. Piskorz, I. Komaromi, R. Gomperts, R. L. Martin, D. J. Fox, T. Keith, M. A. Al-Laham, C. Y. Peng, A. Nanayakkara, C. Gonzalez, M. Challacombe, P. M. W. Gill, B. G. Johnson, W. Chen, M. W. Wong, J. L. Andres, M. Head-Gordon, E. S. Replogle and J. A. Pople, Gaussian, Inc., Pittsburgh PA, 1998.
- [8] D. De Fazio, F. A. Gianturco, J. A. Rodriguez-Ruiz, and K. T. Tang, *J. Phys. B* **27**, 303 (1994).
- [9] H. J. M. Bowen, J. Donohue, D. G. Jenkin, O. Kennard, J. Wheatley, and D. H. Whiffen, “*Tables of Interatomic Distances and Configuration in Molecules and Ions*,” The Chemical Society (London, 1958).
- [10] D. M. Bishop, J. Pipin, and S. M. Cybulski, *Phys. Rev. A* **43**, 4845 (1991).
- [11] G. Maroulis and D. M. Bishop, *Chem. Phys. Lett.* **128**, 462 (1986).
- [12] K. P. Huber and G. Herzberg, “*Molecular Spectra and Molecular Structure Constants of Diatomic Molecules*,” Van Nostrand Reinhold (New York, 1979).
- [13] D. D. Reid and J. M. Wadehra, *Phys. Rev. A* **57**, 2583 (1998).
- [14] J. A. Pople, R. Seeger, and R. Krishnan, *Int. J. Quant. Chem. Symp.* **11**, 149 (1977); R. Krishnan, H. B. Schlegel, and J. A. Pople, *J. Chem. Phys.* **72**, 4654 (1980); K. Raghavachari and J. A. Pople, *Int. J. Quant. Chem.* **20**, 167 (1981).
- [15] W. H. Press, S. A. Teukolsky, W. T. Vetterling, and B. P. Flannery, “*Numerical Recipes in*

- Fortran: The Art of Scientific Computing*,” 2nd. ed., Cambridge University Press (Cambridge, 1992).
- [16] L. I. Schiff, “*Quantum Mechanics*,” 3rd. ed., McGraw-Hill (New York, 1968), Ch. 5.
- [17] K. Smith, “*The Calculation of Atomic Collision Processes*,” John Wiley & Sons (New York, 1971).
- [18] E. Gillman and H. R. Fiebig, *Comput. Phys.* **2**, 62 (1988).
- [19] J. M. Wadehra and S. N. Nahar, *Phys. Rev. A* **36**, 1458 (1987).
- [20] K. R. Hoffman, M. S. Dababneh, Y. -F. Hsieh, W. E. Kauppila, V. Pol, J. H. Smart, and T. S. Stein, *Phys. Rev. A* **25**, 1393 (1982).
- [21] S. Zhou, H. Li, W. E. Kauppila, C. K. Kwan, and T. S. Stein, *Phys. Rev. A* **55**, 361 (1997).
- [22] M. Charlton, T. C. Griffith, G. R. Heyland, and G. L. Wright, *J. Phys. B* **13**, L353 (1980).
- [23] M. Charlton, T. C. Griffith, G. R. Heyland, and G. L. Wright, *J. Phys. B* **16**, 323 (1983).
- [24] A. Deuring, K. Floeder, D. Fromme, W. Raith, A. Schwab, G. Sinapius, P. W. Zitzewitz, and J. Krug, *J. Phys. B* **16**, 1633 (1983).
- [25] D. Fromme, G. Kruse, W. Raith, and G. Sinapius, *J. Phys. B* **21**, L261 (1988).
- [26] P. Ashley, J. Maxom, and G. Laricchia, *Phys. Rev. Lett.* **77**, 1250 (1996).
- [27] J. P. Sullivan, J. P. Marler, S. J. Gilbert, S. J. Buckman, and C. M. Surko, *Phys. Rev. Lett.* **87**, 073201 (2001).

Table I. The values of various parameters used in this work and their sources.

Quantity	Value	Source
bond length	1.401 a_0	[9]
α_d	5.18 a_0^3	[10]
α_d	7.88 a_0^5	[10]
α_o	3.85 a_0^7	[11]
E_{Ps}	8.63 eV	This work
E_{diss}	4.52 eV	[12]
Δ	6.57 eV	This work

Table II. Differential, integrated elastic, and momentum transfer cross sections at selected intermediate impact energies (in atomic units). The notation $a (b)$ means $a \times 10^b$.

Angle (deg.)	50 eV	100 eV	200 eV	300 eV	400 eV	500 eV
0	5.88 (0)	5.23 (0)	3.51 (0)	2.92 (0)	2.38 (0)	2.26 (0)
10	4.40 (0)	3.44 (0)	2.00 (0)	1.69 (0)	1.32 (0)	1.06 (0)
20	2.62 (0)	1.69 (0)	7.63 (-1)	6.01 (-1)	3.92 (-1)	2.88 (-1)
30	1.38 (0)	6.67 (-1)	1.99 (-1)	1.57 (-1)	9.85 (-2)	6.51 (-2)
40	6.09 (-1)	2.04 (-1)	3.79 (-2)	5.22 (-2)	3.72 (-2)	2.96 (-2)
50	2.20 (-1)	5.04 (-2)	5.68 (-3)	2.98 (-2)	2.57 (-2)	2.28 (-2)
60	6.43 (-2)	1.05 (-2)	8.76 (-4)	2.41 (-2)	2.27 (-2)	2.13 (-2)
70	1.44 (-2)	2.42 (-3)	4.03 (-4)	2.19 (-2)	2.16 (-2)	2.10 (-2)
80	2.68 (-3)	1.14 (-3)	3.41 (-4)	2.08 (-2)	2.13 (-2)	2.13 (-2)
90	1.22 (-3)	8.81 (-4)	2.67 (-4)	2.03 (-2)	2.14 (-2)	2.18 (-2)
100	1.40 (-3)	6.88 (-4)	2.02 (-4)	2.01 (-2)	2.17 (-2)	2.23 (-2)
110	1.34 (-3)	5.00 (-4)	1.52 (-4)	2.01 (-2)	2.20 (-2)	2.26 (-2)
120	1.10 (-3)	3.65 (-4)	1.12 (-4)	2.02 (-2)	2.23 (-2)	2.29 (-2)
130	8.23 (-4)	2.69 (-4)	8.55 (-5)	2.03 (-2)	2.26 (-2)	2.30 (-2)
140	5.67 (-4)	2.07 (-4)	6.92 (-5)	2.04 (-2)	2.27 (-2)	2.30 (-2)
150	3.92 (-4)	1.75 (-4)	5.71 (-5)	2.06 (-2)	2.29 (-2)	2.31 (-2)
160	2.93 (-4)	1.60 (-4)	4.85 (-5)	2.07 (-2)	2.29 (-2)	2.30 (-2)
170	2.44 (-4)	1.48 (-4)	4.42 (-5)	2.07 (-2)	2.30 (-2)	2.30 (-2)
180	2.17 (-4)	1.35 (-4)	4.06 (-5)	2.07 (-2)	2.30 (-2)	2.31 (-2)
σ_{elas}	3.37 (0)	1.94 (0)	8.80 (-1)	9.59 (-1)	7.64 (-1)	6.41 (-1)
σ_{mom}	3.92 (-1)	1.57 (-1)	4.79 (-2)	2.95 (-1)	3.01 (-1)	2.96 (-1)

V. FIGURE CAPTIONS

Figure 1. Points on a plane of the configuration used to generate the radial electron charge density of H_2 . The two small circles present the protons in the hydrogen molecule. The large circle represents points on the surface of a sphere of radius r . The dots represent points at which $\rho(\mathbf{r})$ is determined by GAUSSIAN and these values are used to calculate $\rho(\mathbf{r})$ at 40,000 points on the sphere by interpolation. The radial charge density is then determined using Eq. (10).

Figure 2. The present total cross sections for the scattering of low to intermediate energy positrons by H_2 compared with several experimental measurements. The error bars are the “maximum error” as reported by the relevant authors.

Figure 3. The present absorption cross sections for the scattering of positrons by H_2 compared with experimental results. The experimental results are a summation of partial cross section measurements from different experiments. These partial cross sections are for positronium formation by Zhou *et al* [21], first ionization by Maxom *et al* [?], and excitation to the $B^1\Sigma$ state by Sullivan *et al* [27].

Figure 4. The present low-energy differential cross sections for the scattering of positrons by H_2 compared with the *ab initio* calculations of Lino *et al* [1]. The positron energy ranges from 1.36 eV to 6.9 eV.

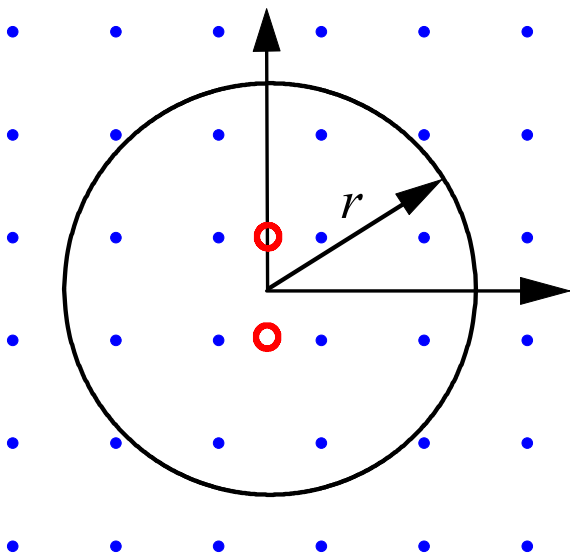


Fig. 1, D. Reid

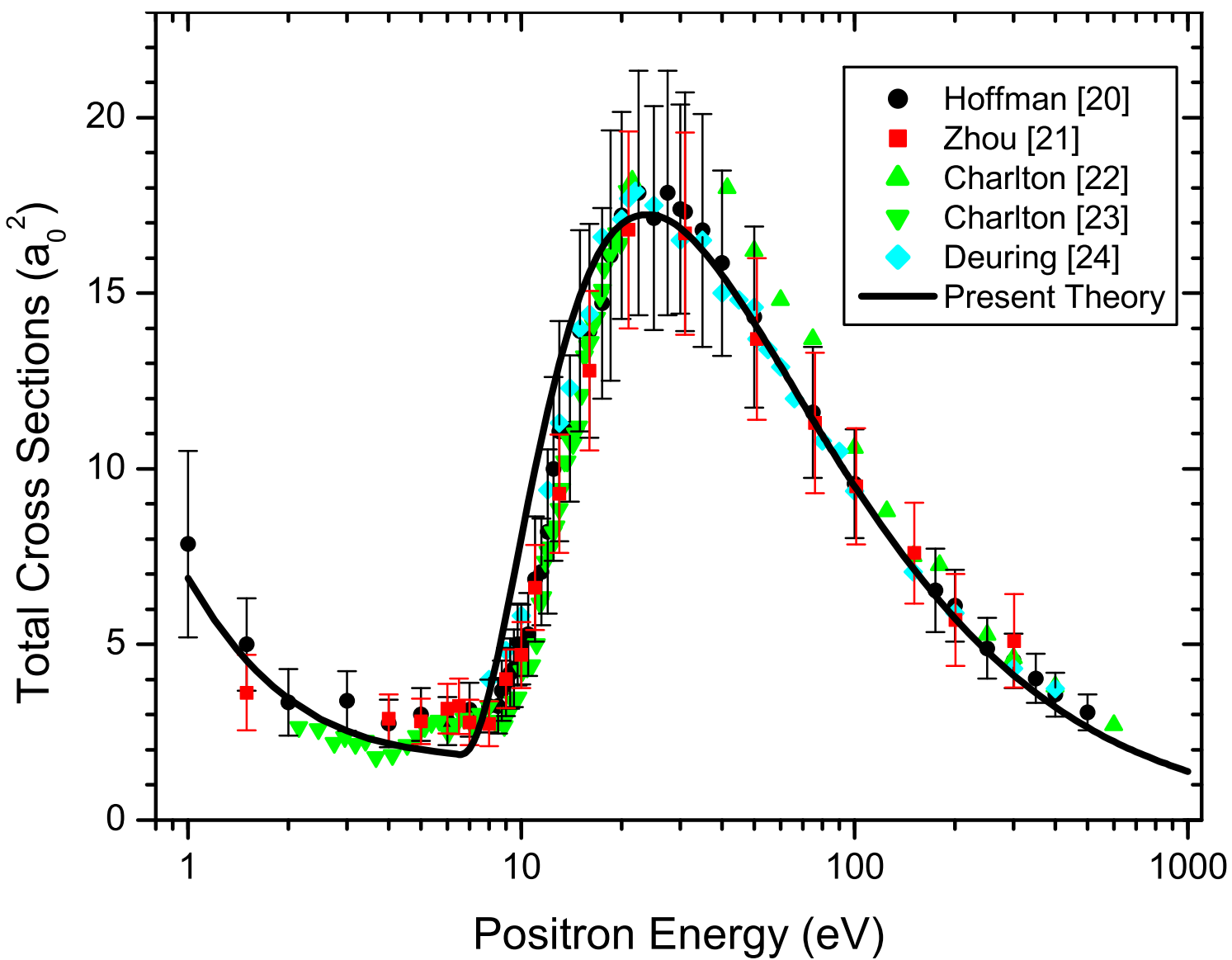


Fig. 2, D. Reid

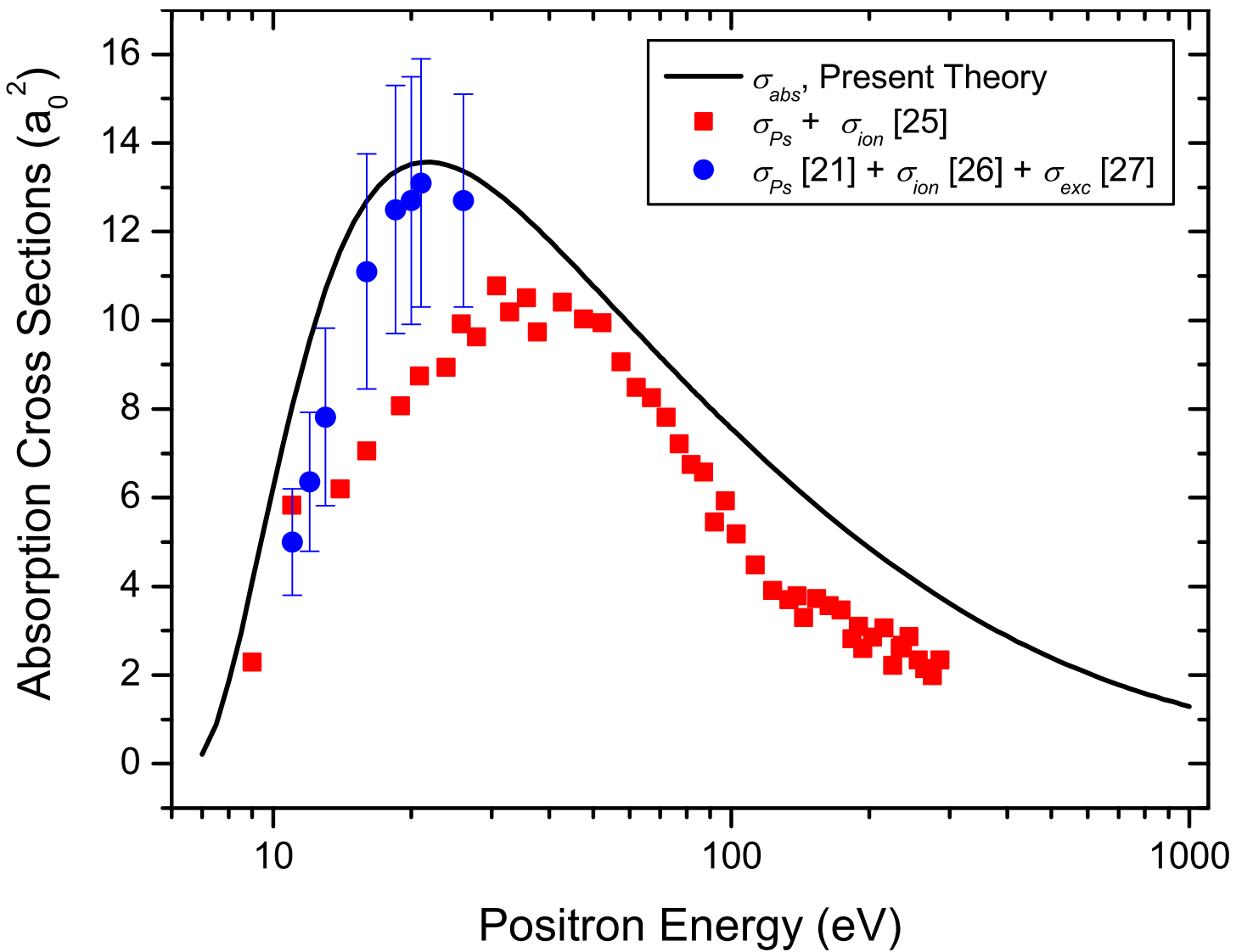


Fig. 3, D. Reid

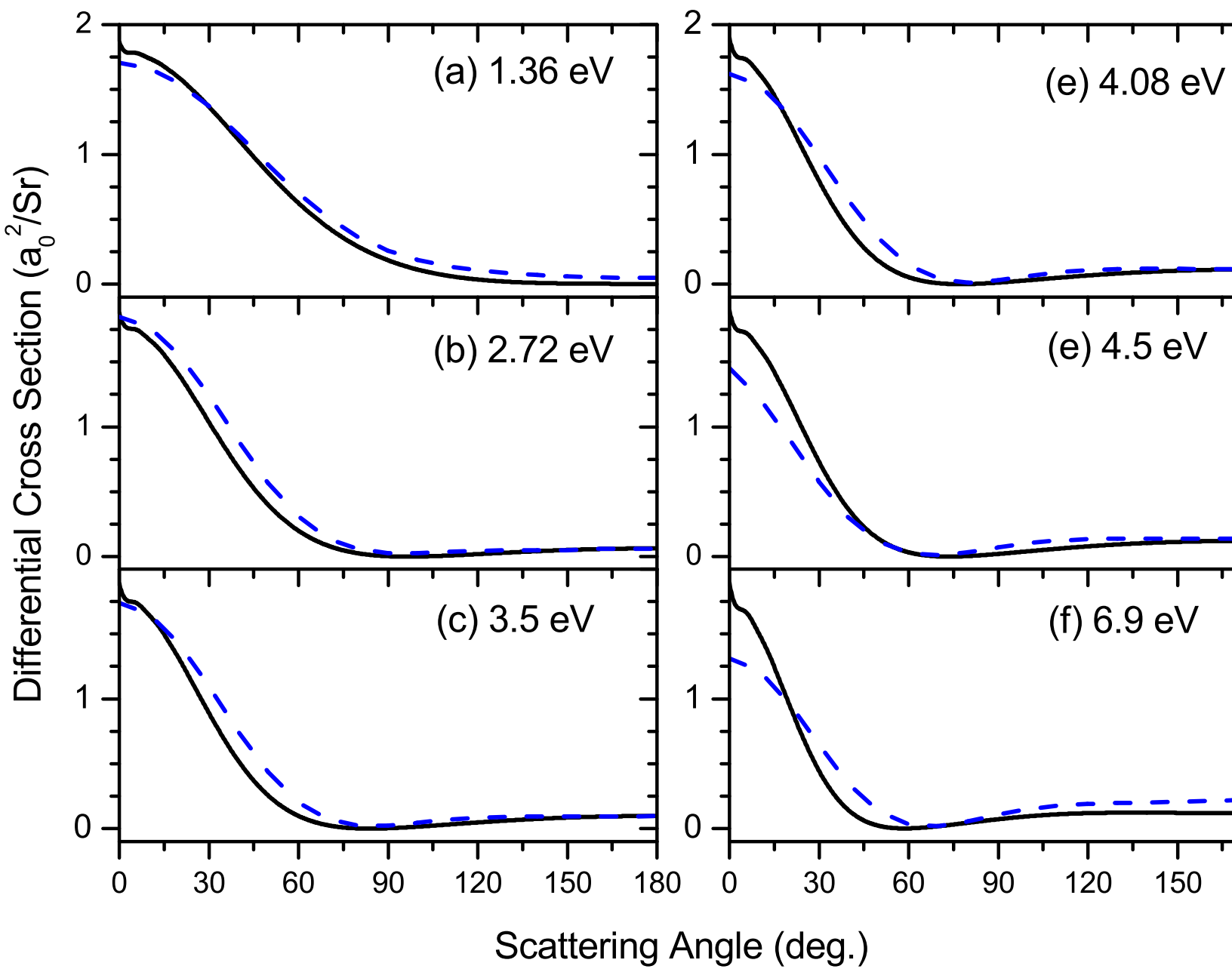


Fig. 4, D. Reid